A Unified Three-Dimensional Trajectory Simulation Methodology

Hideo Ikawa*
Rockwell International, Seal Beach, California

An explicit set of equations of motion described with respect to the flight path coordinate system for the unified three-dimensional trajectory simulation is presented. The theory is uniformly valid for analysis of endo/exo-atmospheric flight problems in which an observer is rotating with the Earth. Hence, the relative properties are taken as the state variables. The rotating spherical coordinate system, which reference plane is oriented with respect to the initial vehicle position and heading, is used. The inverse square gravitational field is assumed. The Coriolis and the centrifugal acceleration terms due to Earth's rotation are also retained. The universal applicability of theory is verified by the sample problems: in-orbit flight; deorbit to land or to perform synergetic plane change, that requires a trans-atmospheric flight maneuver; and low-speed cross-country flight. The theory is suitable for solving such complex problems on a desk-top computer. The sample problems were solved on an IBM PC equipped with an 8087 Numerical Data Processor.

Nomenclature

Az_i	= initial heading azimuth of inertial plane
C_j, F_j	= Coriolis and centrifugal acceleration coefficients due to Earth rotation, j = 1, 2, 3
D, L	= aerodynamic drag and lift
h	= vehicle altitude
i	= trajectory inclination
$\hat{i}$, $\hat{j}$, $\hat{k}$	= unit vectors of reference coordinate system
m	= vehicle mass
r	= radius altitude ($r = h + Re$)
$\hat{r}$, $\hat{e}$, $\hat{n}$	= unit vectors of local coordinate system
Re	= Earth radius
T	= thrust
$\hat{t}_j$	= unit vectors of flight path coordinate system, j = 1, 2, 3
V	= relative speed
Ve	= local Earth rotational speed ($r\ \omega_E \cos\phi_L$)
V_r, V_n, V_t	= velocity components of radial, normal, and tangent to orbit plane
X_E, Y_E, Z_E	= Earth coordinate system
α	= angle of attack
α_T	= engine gimballing angle
β	= bank angle rotating about flight path axes (positive left)
γ	= flight path angle in pitch plane (positive up)
θ	= downrange angle along reference plane
λ, ϕ_L	= longitude and latitude of vehicle position
μ	= universal gravitational constant
ϕ	= crossrange angle normal to reference plane (positive left with respect to initial heading)
ψ	= heading angle with respect to reference plane (positive left with respect to initial heading)
ω	= Earth rotational rate
Ω_o	= nodal point shift measured from X_E (Greenwich)

Subscripts and Superscripts

i	= inertial frame
0	= initial position
1, 2, 3	= vector components
$(\bar{\ })$	= vector
$(\cdot)$	= first derivative with respect to time
$(\cdot\cdot)$	= second derivative with respect to time

Presented as Paper 85-1821 at the AIAA 12th Atmospheric Flight Mechanics Conference, Snowmass, CO, Aug. 19–21, 1985; received Sept. 16, 1985; revision received Feb. 24, 1986.

*Member Technical Staff. Currently no affiliation. Member AIAA.

Introduction

AN advent of the successful flights of the Space Shuttle, the flights of winged spacecraft in the interfacing regime of endo/exo-atmosphere, which were prematurely explored in the 1960s, are becoming maturity. The concepts of aeroassisted orbital transfer vehicles, reentry research vehicles, and hypersonic boost glide/cruise vehicles are now blossoming into realities. For a mission scenario, an analyses of a complete trajectory cycle of specific mission profile is needed. The POST,[1] the well accepted trajectory simulation program coded on CDC CYBER, is used extensively for this purpose. However, for preliminary studies, a less sophisticated but a reliable and user-friendly computer program is desirable.

With a suitable theory, the appearance of desk-top computers with a highly advanced capability has made possible the quick trajectory simulation without relying upon a large computer. For the three-dimensional equations of motion given in the past, however, the reference plane is fixed on the equatorial plane (for example, Ref. 2). The inconvenience of this formulation is that the downrange and crossrange measurements cannot be related directly to the initial position, unless the vehicle departs from the equator.

An explicit expression of unified three-dimensional trajectory simulation methodology given with respect to the flight path coordinate system, that meets the requirements for desk-top computers and for a direct range computation, is formulated. The theory offers a physical insight into the problem without requiring additional coordinate transformations. A spherical coordinate system fixed on the rotating earth, with its reference plane oriented with respect to the initial vehicle position and heading, is used as the reference system. An inverse square gravitational field is assumed. The derived set of equations of motion reduces to the definition of Keplerian orbit mechanics when the effects of aerodynamic and thrust diminish. The method is hence uniformly valid for evaluating the entire planetary flight continuously through the atmosphere and the space.

Equations of Motion

The primary interest is concentrated on the trajectory simulation of aerodynamically and propulsively maneuverable vehicles operating in the endo/exo-atmosphere. Therefore, the full equations of motion for hypersonic flight are included without any compromise. However, the methodology can be applied equally for the

low-speed flight simulation—an evaluation of a commercial flight from Los Angeles to New York on a 747, for example.

The well established vector equation which describes the motion of a point mass measured with respect to the fixed reference system on a rotating planet[2,3] is given as

$$\frac{d\bar{V}}{dt} = \frac{\bar{F}}{m} - 2\bar{\omega} \times \bar{V} - \bar{\omega} \times (\bar{\omega} \times \bar{r}) \tag{1}$$

The velocity ($\bar{V}$) is taken relative to the planet and the time derivatives are taken with respect to the planet fixed axes. The first term ($\bar{F}$) on the right-hand side (RHS) represents the applied external forces produced by gravitational field, aerodynamics and propulsion system. The last two terms are induced by the planet's rotation in which the second term, a Coriolis acceleration, contributes to a high-speed, long-range flight. The last term on RHS, a centrifugal acceleration, is usually neglected in the atmospheric flight but plays an important role in the orbital trajectory simulation.

The planet fixed reference coordinate system is shown in Fig. 1. The reference plane, defined by the initial vehicle position and heading (i_0, Ω_0, θ_0), forms a great circle with respect to the geopotential center and is inclined with respect to the planet's equator. The position and velocity vectors in the reference frame are given as

$$\bar{r} = (r_1, r_2, r_3) \tag{2}$$

$$\bar{V} = \dot{\bar{r}} = (\dot{r}_1, \dot{r}_2, \dot{r}_3) \tag{3}$$

The downrange and crossrange measurements from the initial point along and normal to the reference plane are defined by angular distances (θ, ϕ) taken with respect to the geopotential center, respectively. Hence, the position components for Eq. (2) can be described by (see Fig. 2)

$$r_1 = r\cos\phi\cos\theta \qquad r_2 = r\cos\phi\sin\theta \qquad r_3 = r\sin\phi \tag{4}$$

The projected position on the planet's surface is defined by letting $r = Re$.

The kinematic relation is derived by following step. From Fig. 2, the definition of velocity can be expressed in a local coordinate system ($\hat{r}$, $\hat{e}$, $\hat{n}$) in terms of state derivatives and also in terms of vehicle heading (ψ) and flight path angles (γ).

$$\bar{V} = \frac{dr}{dt}\hat{r} + r\cos\phi\frac{d\theta}{dt}\hat{e} + r\frac{d\phi}{dt}\hat{n} \tag{5}$$

$$\bar{V} = V\sin\gamma\,\hat{r} + V\cos\gamma\cos\psi\,\hat{e} + V\cos\gamma\sin\psi\,\hat{n} \tag{6}$$

The kinematic relation is expressed by equating Eqs. (5) and (6).

$$\frac{dr}{dt} = V\sin\gamma$$

$$\frac{d\theta}{dt} = \frac{V\cos\gamma\cos\psi}{r\cos\phi}$$

$$\frac{d\phi}{dt} = \frac{V\cos\gamma\sin\psi}{r} \tag{7}$$

The final momentum equations expressed in the flight path coordinate system are summarized. The derivation is discussed in the Appendices.

$$\frac{dV}{dt} = \frac{T\cos(\alpha_T + \alpha) - D}{m} - \frac{\mu\sin\gamma}{r^2} + r\,\omega_E^2 F_1 \tag{8a}$$

$$\frac{V d\gamma}{dt} = \frac{[T\sin(\alpha_T + \alpha) + L]\cos\beta}{m} - \left(\frac{\mu}{n^2} - \frac{V^2}{n}\right)\cos\gamma + 2V\,\omega_E C_2 + r\,\omega_E^2 F_2 \tag{8b}$$

$$V\cos\gamma\frac{d\psi}{dt} = \frac{[T\sin(\alpha_T + \alpha) + L]\sin\beta}{m} - \frac{V^2\cos^2\gamma\cos\psi\tan\phi}{r} - 2V\,\omega_E C_3 - r\,\omega_E^2 F_3 \tag{8c}$$

where the Coriolis acceleration coefficients which contribute to pitch and yaw components are given as

$$C_2 = \cos i_0\cos\phi\cos\psi - \sin i_0[\sin\psi\cos(\theta_0 + \theta) + \cos\psi\sin\phi\sin(\theta_0 + \theta)] \tag{9a}$$

$$C_3 = \cos i_0(\cos\gamma\sin\phi - \sin\gamma\cos\phi\sin\psi) + \sin i_0[(\cos\gamma\cos\phi + \sin\gamma\sin\phi\sin\psi)\sin(\theta_0 + \theta) - \sin\gamma\cos\psi\cos(\theta_0 + \theta)] \tag{9b}$$

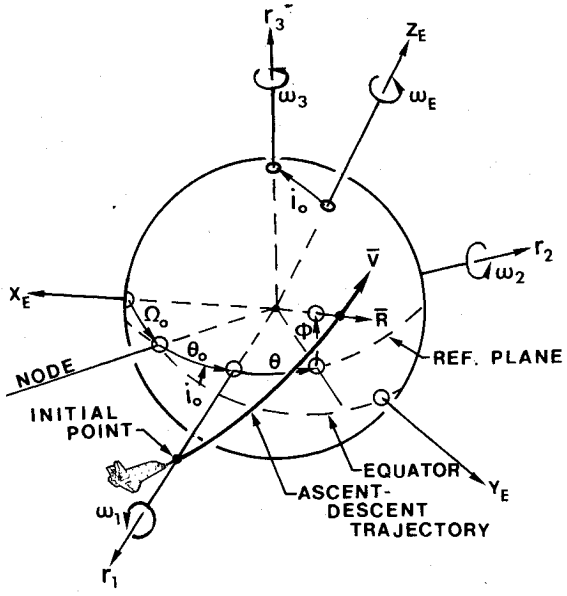

Fig. 1 Earth and reference coordinate systems.

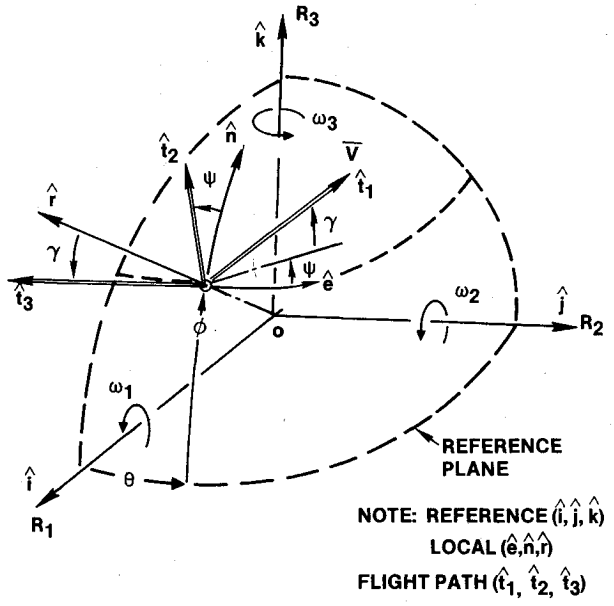

Fig. 2 Reference, local and flight path coordinate systems.

The centrifugal acceleration coefficients are given as

$$F_1 = [\cos^2 i_0 + \sin^2 i_0 \cos^2(\theta_0 + \theta)] \times \cos\phi\,(\sin\gamma\cos\phi - \cos\gamma\sin\phi\sin\psi) + \sin^2 i_0\,[\sin\phi\,(\sin\gamma\sin\phi + \cos\gamma\cos\phi\sin\psi) - \cos\gamma\cos\phi\cos\psi\cos(\theta_0 + \theta)\sin(\theta_0 + \theta)] - \sin i_0\cos i_0\,[(2\sin\gamma\sin\phi\cos\phi + \cos\gamma\sin\psi\cos 2\phi)\sin(\theta_0 + \theta) + \cos\gamma\cos\psi\sin\phi\cos(\theta_0 + \theta)] \quad (10a)$$

$$F_2 = [\cos^2 i_0 + \sin^2 i_0 \cos^2(\theta_0 + \theta)] \times \cos\phi\,(\cos\gamma\cos\phi + \sin\gamma\sin\phi\sin\psi) + \sin^2 i_0[\sin\phi\,(\cos\gamma\sin\phi - \sin\gamma\cos\phi\sin\psi) + \sin\gamma\cos\phi\cos\psi\cos(\theta_0 + \theta)\sin(\theta_0 + \theta)] + \sin i_0\cos i_0\,\{\sin\gamma\sin\phi\cos\psi\cos(\theta_0 + \theta) + [\sin\gamma\sin\psi - 2\sin\phi\,(\cos\gamma\cos\phi + \sin\gamma\sin\phi\sin\psi)]\sin(\theta_0 + \theta)\} \quad (10b)$$

$$F_3 = \cos^2 i_0\sin\phi\cos\phi\cos\psi - \sin^2 i_0\cos\phi\,[\sin\psi\sin(\theta_0 + \theta)\cos(\theta_0 + \theta) + \sin\phi\cos\psi\sin^2(\theta_0 + \theta)] + \sin i_0\cos i_0\,[\cos\psi\cos 2\phi\sin(\theta_0 + \theta) - \sin\phi\sin\psi\cos(\theta_0 + \theta)] \quad (10c)$$

For the propulsive stage, the rate of decrease of vehicle mass is determined by thrust T and specific impulse I_{sp}.

$$\frac{dm}{dt} = \frac{-\text{abs}(T)}{I_{sp}} \quad (11)$$

The trajectory inclination angle changes only when the aerodynamic and/or propulsive forces are applied in the lateral plane of motion. The rate of change of inclination[4] is expressed as

$$\frac{di}{dt} = \frac{\cos Az_i\cos\phi_L}{\sin i}\left(\frac{d\psi}{dt}\right)_{EF} \quad (12)$$

where $(d\psi/dt)_{EF}$ is defined by the first RHS term of Eq. (8c) and Az_i by the known inclination and latitude using the right spherical triangle relationship

$$\sin Az_i = \frac{\cos i}{\cos\phi_L} \quad (13)$$

The vehicle position can be described in the terms of latitude and longitude of planet by the following transformations:

$$\sin\phi_L = \sin\phi\cos i_0 + \cos\phi\sin(\theta_0 + \theta)\sin i_0 \quad (14a)$$

$$\tan\lambda = \frac{P1\sin\Omega_0 + P2\cos\Omega_0}{P1\cos\Omega_0 - P2\sin\Omega_0} \quad (14b)$$

where

$$P1 = \cos\phi\cos(\theta_0 + \theta)$$

$$P2 = \cos\phi\sin(\theta_0 + \theta)\cos i_0 - \sin\phi\sin i_0$$

One can verify that $\phi_L = \phi$ and $\lambda = \Omega_0 + \theta_0 + \theta$ only when $i_0 = 0$.

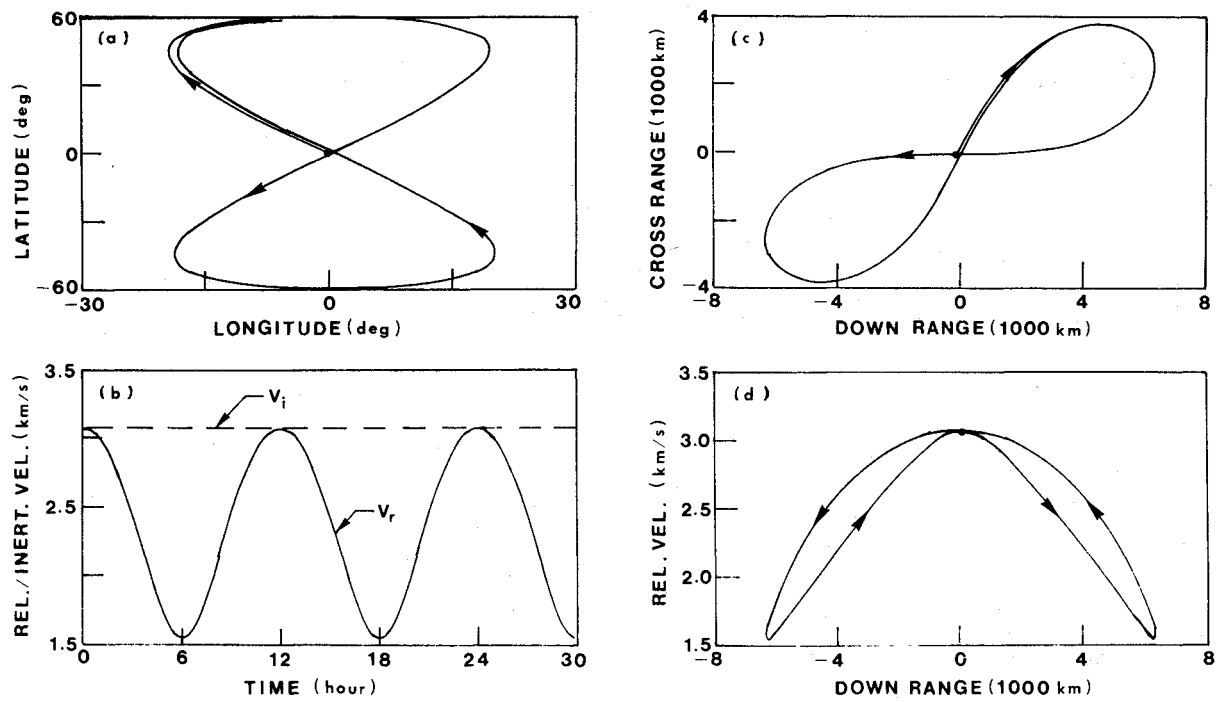

Fig. 3 24-h circular orbit, $i_0 = 60$ deg: a) ground trace; b) inertial/relative velocity histories; c) crossrange vs downrange; d) relative velocity vs downrange.

The initial conditions of a vehicle position and its states are given as

$$i = i_0, \quad \phi_L = \phi_{L0}, \quad \lambda = \lambda_0 \text{ (inclination, latitude, longitude)}$$

$$V = V_0, \quad \gamma = \gamma_0,$$

$$h = h_0 \text{ (velocity, flight path angle, altitude)}$$

$$\psi = 0, \quad \theta = 0,$$

$$\phi = 0 \text{ (heading, downrange, crossrange angles)}$$

The variable control parameters are angle of attack, bank angle, thrust angle, thrust and specific impulse (α, β, α_T, T, I_{sp}). The reader should note that the initial heading angle is normally zero because the vehicle is initially aligned with respect to the reference plane defined by the inclination, i_0. However, for a trajectory starting from the space, the initial relative heading angle is computed by the inertial properties as will be shown in the next section.

Equations (4) and (7–14) and the initial conditions completely describe the problem. The problem is solved by the shooting method. The desired solution is obtained by adjusting the initial conditions and/or variable control parameters at the staging points. The fourth-order Runge-Kutta routine suitable for the personal computer is used to integrate the preceding set of equations.

Inertial and Relative Velocity Relationship

For the reference plane aligned with the equator, the universal nature of the equations can be immediately verified by setting $i_0 = 0$ in Eqs. (9) and (10). In this case, the endo-atmospheric equations given in Ref. 2 are reproduced. For a vanishing contribution of aerodynamics and propulsive forces, the equations reduce to two-dimensional Keplerian mechanics.

For a nonequatorial reference plane, however, the reduction of equations in the form of Keplerian mechanics is not obvious because of the cross-term, $\sin i_0 \cos i_0$. In this case, a numerical verification is performed. Recall, the equations are derived using a relative velocity ($\bar{V}$) with respect to the rotating planet. Therefore, the relationship between the relative ($\bar{V}$) and the given inertial ($\bar{V}_i$) velocities at the initial point is required for the orbit problem. Then a nonzero initial relative heading angle is defined.

For the given initial inertial velocity and flight path angle, the tangential and radial velocity components are defined as

$$V_{ti} = V_i \cos\gamma_i, \quad V_{ri} = V_i \sin\gamma_i \tag{15}$$

The local Earth rotational speed at the given latitude ϕ_L is

$$Ve = r\,\omega_E \cos\phi_L \tag{16}$$

The tangential and normal relative velocity components with respect to the orbit plane are

$$V_t = (V_{ti}^2 - 2V_{ti}\, r\, \omega_E \cos i_0 + V_e^2)^{1/2} \tag{17}$$

$$V_n = V_{ti} \sin Az_i - Ve \tag{18}$$

The magnitude of relative velocity and flight path angle are

$$V = (V_t^2 + V_{ri}^2)^{1/2} \tag{19}$$

$$\gamma = \arcsin(V_{ri}/V) \tag{20}$$

The initial relative heading angle (ψ_0) between the inertial and the relative trajectories is defined by

$$\psi_0 = Az_i - \arcsin(V_n/V_t) \tag{21}$$

where Az_i is the heading azimuth of the inertial orbit plane at the initial vehicle position computed by Eq. (13), letting $i = i_0$.

Discussion of Results

Several sample cases are demonstrated to verify the universal nature of the derived equations. The sample computations were performed on an IBM PC equipped with a 8087 Numeric Data Processor. The typical trajectories were computed in 3 to 5 min for in-orbit, 15 to 18 min for deorbit to land or for synergetic plane change, and 30 min for low-speed cross-country cases.

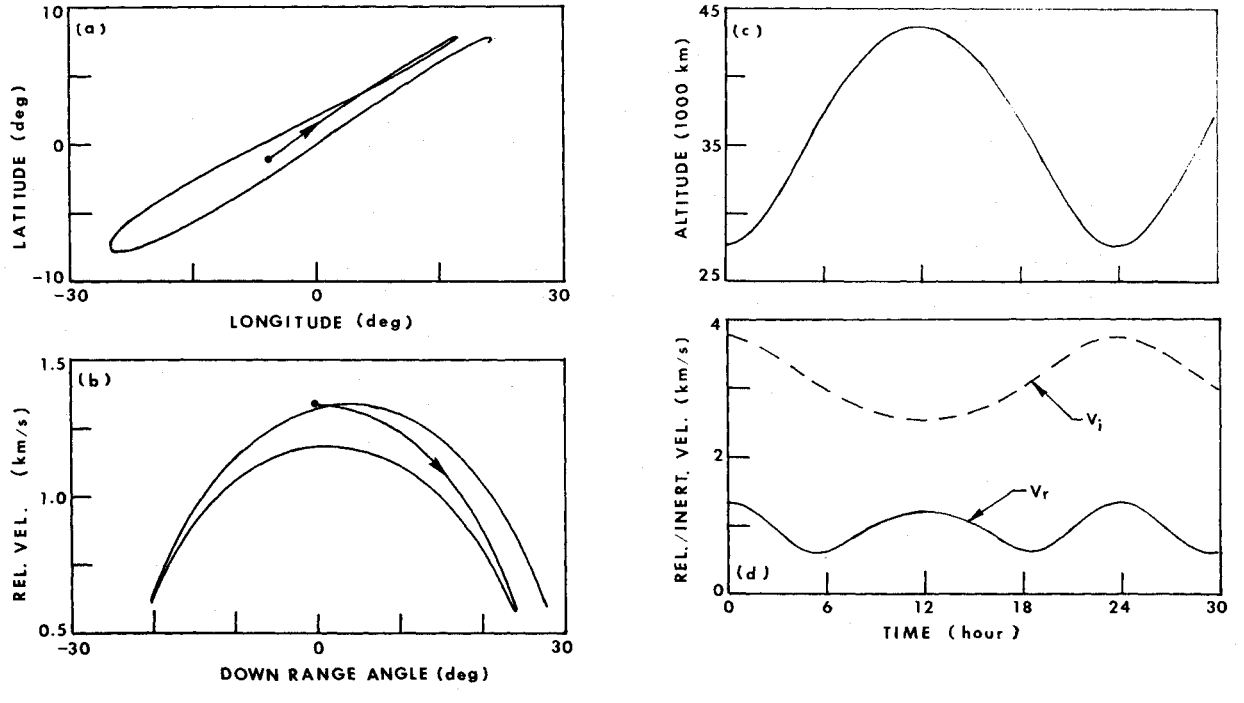

Fig. 4 23.6-h elliptic orbit, $i_0 = 7.778$ deg, $h_p = 27{,}243$ km, $h_a = 42{,}705$ km: a) ground trace; b) relative velocity vs downrange angle; c) altitude history; d) inertial/relative velocity histories.

To demonstrate that the set of equations reduces to Keplerian mechanics, a satellite on a nonequatorial circular orbit at the geosynchronous altitude is computed. It forms a figure eight (8) ground trace.[5] This is verified for the 24-h orbit with 60-deg inclination as shown in Fig. 3a. Although the inertial velocity of a circular orbit is invariant, the relative velocity varies with the latitude position which depicts a 12-h cycle as shown in Fig. 3b. The crossrange and velocity vs downrange are shown in Figs. 3c and 3d, respectively.

An elliptic orbit (e = .187) with an anomalistic period of 23.6 h inclined at 7.778 deg[5] is simulated. The ground trace in Fig. 4a shows a typical figure eight with the nodal shift per cycle because the orbit is not precisely 24 h. The velocity versus downrange is shown in Fig. 4b. The approximate 24-h cycle of altitude traverse is given in Fig. 4c. Although the inertial velocity is inversely proportional to the altitude cycle in Fig. 4d, the relative velocity follows the cycle with respect to the latitude position.

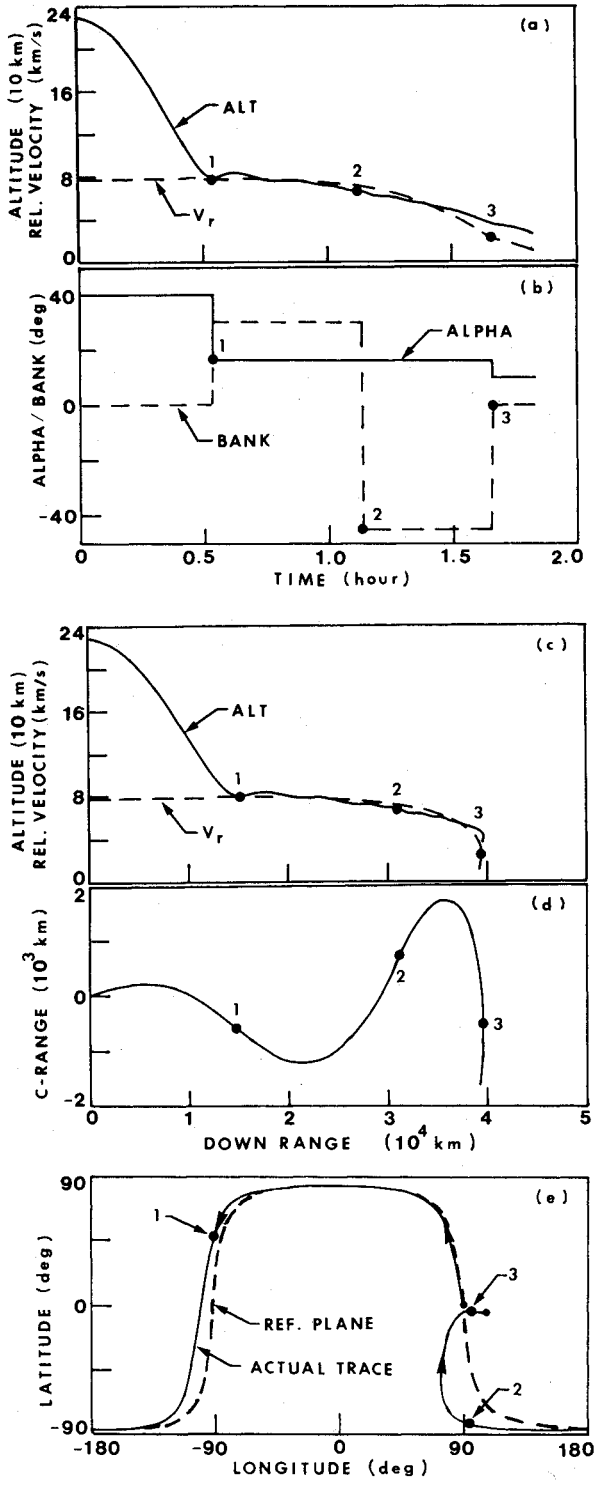

Fig. 5 Deorbit to land from elliptic LEO, i_0 = 96.2 deg, t_0 = 97.3 min, h_{p0} = 225 km, h_{a0} = 1012 km. a) altitude–relative velocity histories; b) angle of attack–bank angle histories; c) altitude–relative velocity vs downrange; d) crossrange vs downrange; e) ground trace.

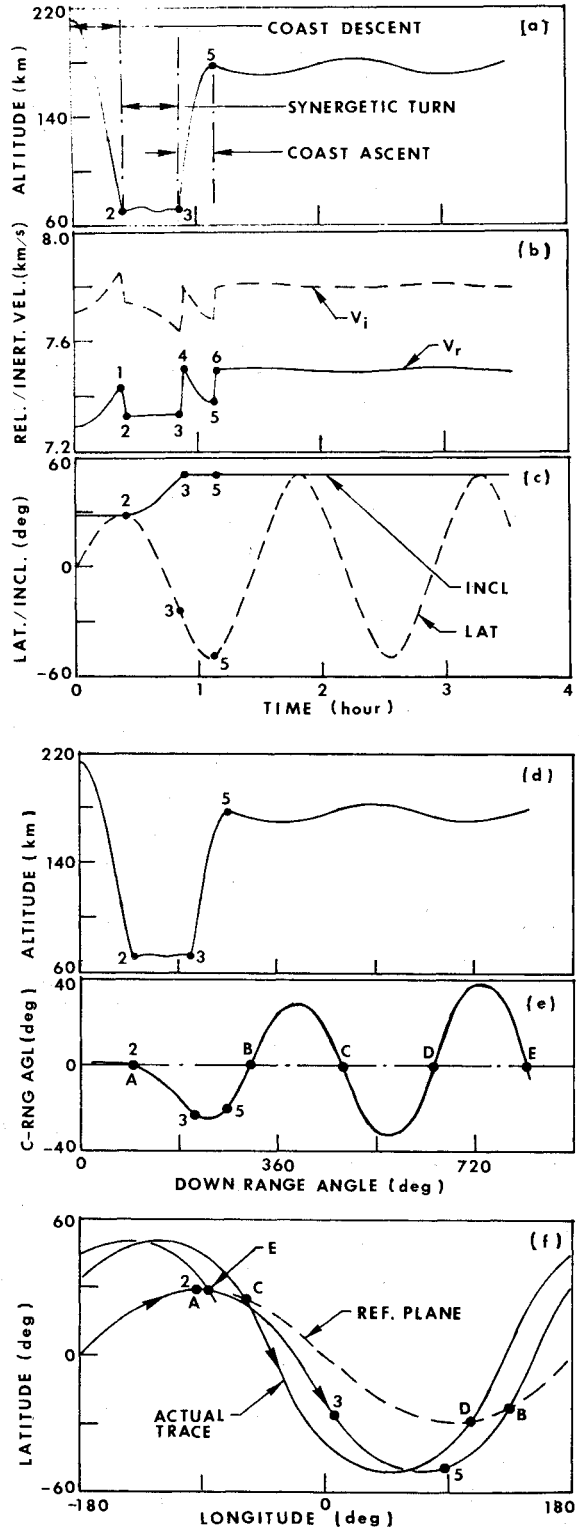

Fig. 6 Synergetic plane change, h_0 = 212 km, i_0 = 28.5 deg; h_f = 180 km, i_f = 52 deg. a) altitude history; b) inertial/relative velocity histories; c) inclination–latitude histories; d) altitude vs downrange angle; e) crossrange vs downrange angles; f) ground trace.

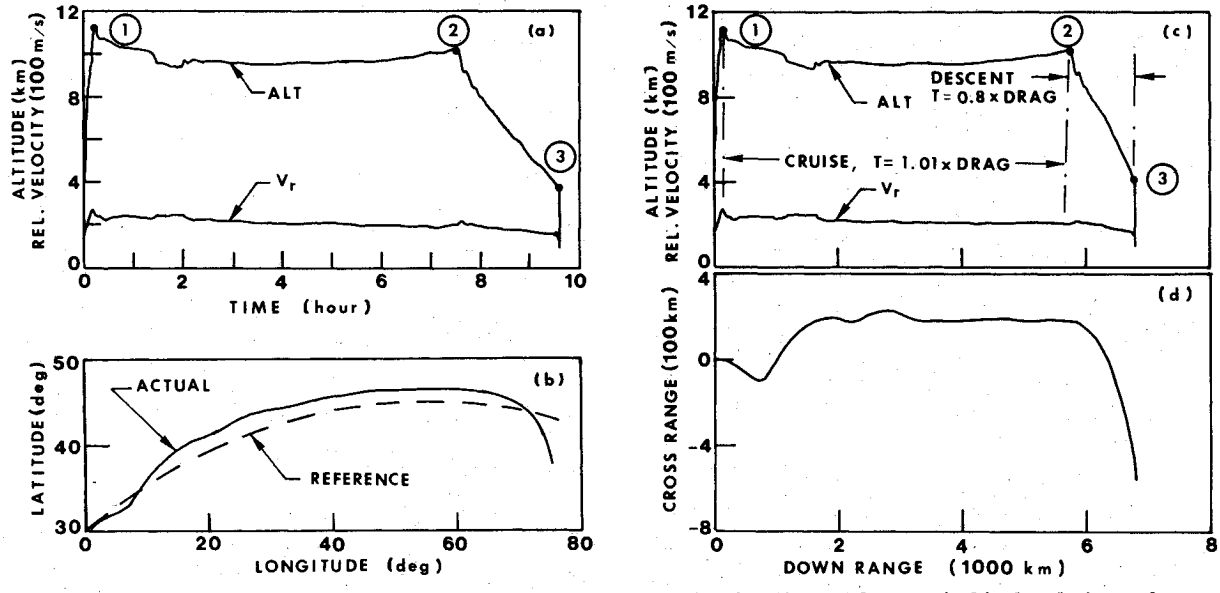

Fig. 7 Low-speed cross-country flight (East), $i_0 = 45$ deg: a) altitude-velocity histories; b) ground trace; c) altitude-velocity vs downrange; d) crossrange vs downrange.

To demonstrate the re-entry analysis capability, the deorbit burn ($\Delta V = -305$ m/s) was applied at the perigee of an elliptic low Earth orbit (LEO) in near polar orbit with 96.2-deg inclination.[5] Both 30- and −45-deg bank turns (as marked numerically in figures) were used for the endo-atmospheric maneuver to establish the crossrange. The altitude and relative velocity histories are shown in Fig. 5a and the angle of attack/bank angle modulation histories in Fig. 5b. The altitude and velocity vs downrange of Fig. 5c can be overlayed on Fig. 5d (crossrange vs downrange) to depict the three-dimensional trajectory profile. The −45-deg bank angle was executed at the final northbound leg of trajectory (point 2) to bring the vehicle back near the equator as shown in the ground trace (Fig. 5f).

The synergetic orbit plane change is simulated next. The altitude history is shown in Fig. 6a, the inertial and relative velocities in Fig. 6b, and the trajectory inclination and latitude in Fig. 6c. The altitude and crossrange vs downrange are shown in Figs. 6d and 6e. The points of interest are listed numerically. The initial aerodynamic deceleration occurred between points 1 and 2 during the entry and descent phase. Because the synergetic inclination change is most effectively accomplished near the equator crossing,[4] the aero-turning maneuver was initiated near the upper apex (point 2) and completed before the lower apex (point 3) of trajectory as shown in Fig. 6f. It was performed with a throttlable rocket ($T = 1.1 \times$ drag) and with the vehicle attitude trimmed at a 24-deg angle of attack and a −85-deg bank [on the southbound leg of trajectory, the right turn increases the trajectory inclination (Ref. 4)]. The reorbit burn was applied between points 3 and 4. The vehicle coasted to point 5 where the insertion burn was made. The 28.5-deg orbit plane was changed to the 52-deg inclined orbit with a total delta-V expenditure of 2009 m/s. The points where the revised trajectory crossed the reference plane are shown alphabetically in Figs. 6e and 6f.

The final demonstration is a simulation of low-speed cross-country trip on a commercial aircraft. The altitude and velocity histories are given in Fig. 7a and the ground trace in Fig. 7b. The altitude–velocity and crossrange vs downrange are given in Figs. 7c and 7d. The computation simulates a horizontal take-off and climb to a cruise altitude of approximately 11.2 km (point 1) at Mach 0.8. During the cruise, the thrust is maintained at $1.01 \times$ drag. The cruise altitude decays initially until the vehicle becomes lighter as the propellent is consumed. At point 2, the throttle is pulled back to $0.8 \times$ drag to descend. The allocated propellent has been exhausted at point 3, the aircraft's approach angle becomes excessive, and it crashes. In order to counter-balance the Coriolis force, the vehicle requires very slight left-hand banking (0 to 0.1 deg bank) to maintain its heading. The reference trajectory is taken along the eastbound heading described by an $i_0 = 45$-deg inclination (dashed-line, Fig. 7b). The midcourse heading changes are interactively applied.

Conclusions

A useful, explicit form of equations of motion which offers a physical insight into the three-dimensional trajectory simulation, without requiring additional coordinate transformations, is presented in this paper. The theory is uniformly valid for continuous analysis of endo/exo-atmospheric flight problems on a rotating planet. The spherical coordinate system is used and the inverse square gravitational field is assumed. The set of equations is suitable for coding on the desk-top computers for accurate, preliminary trajectory simulation. An advantage of the desk-top computers is that an autonomous interactive capability can be incorporated to change control parameters, such as angles of attack, bank angle, propulsion setting, etc., during the computation.

Many different types of trajectories can be simulated in which capability will be dependent upon the user's ingenuity to code such cases. Sample problems of in-orbit; deorbit to land and to perform synergetic plane change, that require a trans-atmospheric flight maneuver; and low-speed cross-country flight are demonstrated to verify the universal nature of this theory.

Appendix A: Components in Reference Coordinate System

The formulation of momentum equations [Eqs. (8–10)] is briefly discussed. The unit vector triads for the local and reference system are related by the following transformations from Fig. 2:

$$\begin{aligned}\hat{r} &= \cos\phi\cos\theta\,\hat{i} + \cos\phi\sin\theta\,\hat{j} + \sin\phi\,\hat{k}\\ \hat{e} &= -\sin\theta\,\hat{i} + \cos\theta\,\hat{j}\\ \hat{n} &= -\sin\phi\cos\theta\,\hat{i} - \sin\phi\sin\theta\,\hat{j} + \cos\phi\,\hat{k}\end{aligned} \qquad \text{(A1)}$$

Substituting Eq. (A1) into Eq. (6), velocity components in the form of Eq. (3) can be expressed as

$$\dot{r}_1 = V[\cos\phi\cos\theta\sin\gamma - (\sin\psi\sin\phi\cos\theta + \cos\psi\sin\theta)\cos\gamma]$$

$$\dot{r}_2 = V\,[\cos\phi\sin\theta\sin\gamma - (\sin\psi\sin\phi\sin\theta - \cos\psi\cos\theta)\cos\gamma]$$

$$\dot{r}_3 = V\,(\sin\phi\sin\gamma + \sin\psi\cos\phi\cos\gamma) \tag{A2}$$

The scalar accelerations in terms of derivatives of state variables can be derived by differentiating Eq. (A2).

$$\begin{aligned}\ddot{r}_1 = {} & (\dot{V}/V)\dot{r}_1 + V\dot{\gamma}\,[\cos\phi\cos\theta\cos\gamma \\ & + (\cos\psi\sin\theta + \sin\psi\sin\phi\cos\theta)\sin\gamma] \\ & - V\dot{\phi}\,(\sin\phi\cos\theta\sin\gamma + \sin\psi\cos\phi\cos\theta\cos\gamma) \\ & + V\dot{\psi}\,[(\sin\psi\sin\theta - \cos\psi\sin\phi\cos\theta)\cos\gamma] \\ & - V\dot{\theta}\,[\cos\phi\sin\theta\sin\gamma \\ & + (\cos\psi\cos\theta - \sin\psi\sin\phi\sin\theta)\cos\gamma]\end{aligned} \tag{A3a}$$

$$\begin{aligned}\ddot{r}_2 = {} & (\dot{V}/V)\dot{r}_2 + V\dot{\gamma}\,[\cos\phi\sin\theta\cos\gamma \\ & - (\cos\psi\cos\theta - \sin\psi\sin\phi\sin\theta)\sin\gamma] \\ & - V\dot{\phi}\,(\sin\phi\sin\theta\sin\gamma + \sin\psi\cos\phi\sin\theta\cos\gamma) \\ & - V\dot{\psi}\,[(\sin\psi\cos\theta + \cos\psi\sin\phi\sin\theta)\cos\gamma] \\ & + V\dot{\theta}\,[\cos\phi\cos\theta\sin\gamma \\ & - (\cos\psi\sin\theta + \sin\psi\sin\phi\cos\theta)\cos\gamma]\end{aligned} \tag{A3b}$$

$$\begin{aligned}\ddot{r}_3 = {} & (\dot{V}/V)\dot{r}_3 \\ & + V\dot{\gamma}\,(\sin\phi\cos\gamma - \sin\psi\cos\phi\sin\gamma) \\ & + V\dot{\phi}\,(\cos\phi\sin\gamma - \sin\psi\sin\phi\cos\gamma) \\ & + V\dot{\psi}\cos\psi\cos\phi\cos\gamma\end{aligned} \tag{A3c}$$

The rate of planet rotation vector in the reference frame can be easily shown as

$$\bar{\omega} = (\omega_1, \omega_2, \omega_3)$$

where

$$\begin{aligned}\omega_1 &= \omega_E \sin i_0 \sin\theta_0 \\ \omega_2 &= \omega_E \sin i_0 \cos\theta_0 \\ \omega_3 &= \omega_E \cos i_0\end{aligned} \tag{A4}$$

The Coriolis and centrifugal accelerations can be re-expressed as

$$\bar{\omega} \times \bar{V} = (CE_1, CE_2, CE_3) \tag{A5}$$

$$\bar{\omega} \times (\bar{\omega} \times \bar{r}) = (CF_1, CF_2, CF_3) \tag{A6}$$

where

$$\begin{aligned}CE_i &= \omega_j \dot{r}_k - \omega_k \dot{r}_j \\ CF_i &= \omega_i(\omega_j r_j + \omega_k r_k) - r_i(\omega_j^2 + \omega_k^2)\end{aligned}$$

and i, j, k are cyclic as $i = 1, 2, 3$; $j = 2, 3, 1$; $k = 3, 1, 2$.

Then Eq. (1) without the external force term can be rewritten in components of the reference coordinate system by using the definitions of Eqs. (A3, A5, and A6).

$$\ddot{\bar{r}} = -2\overline{CE} - \overline{CF} \tag{A7}$$

Appendix B: Unit Vectors in Flight Path Coordinate System

After performing successive coordinate transformations, the unit vector triad described in the flight path coordinate system (right hand rule) can be expressed in terms of the reference axes unit vectors. The unit vector, $\hat{t}_1$, in the direction of flight is given as

$$\begin{aligned}\hat{t}_1 = {} & \hat{i}\,[\cos\phi\cos\theta\sin\gamma \\ & - (\cos\psi\sin\theta + \sin\psi\sin\phi\cos\theta)\cos\gamma] \\ & + \hat{j}\,[\cos\phi\sin\theta\sin\gamma \\ & + (\cos\psi\cos\theta - \sin\psi\sin\phi\sin\theta)\cos\gamma] \\ & + \hat{k}\,(\sin\phi\sin\gamma + \sin\psi\cos\phi\cos\gamma)\end{aligned} \tag{B1a}$$

The unit vectors in the directions of yaw (left as positive) and pitch (up as positive) planes are

$$\begin{aligned}\hat{t}_2 = {} & \hat{i}\,(\sin\psi\sin\theta - \cos\psi\sin\phi\cos\theta) \\ & - \hat{j}\,(\sin\psi\cos\theta + \cos\psi\sin\phi\sin\theta) + \hat{k}\cos\psi\cos\phi\end{aligned} \tag{B1b}$$

$$\begin{aligned}\hat{t}_3 = {} & \hat{i}\,[\cos\phi\cos\theta\cos\gamma \\ & + (\cos\psi\sin\theta + \sin\psi\sin\phi\cos\theta)\sin\gamma] \\ & + \hat{j}\,[\cos\phi\sin\theta\cos\gamma \\ & - (\cos\psi\cos\theta - \sin\psi\sin\phi\sin\theta)\sin\gamma] \\ & + \hat{k}\,(\sin\phi\cos\gamma - \sin\psi\cos\phi\sin\gamma)\end{aligned} \tag{B1c}$$

Also note that, from comparison of Eq. (A2) and (B1a), $\hat{t}_1$ can be also expressed as

$$\hat{t}_1 = \frac{(\dot{r}_1\hat{i} + \dot{r}_2\hat{j} + \dot{r}_3\hat{k})}{V} \tag{B2}$$

Therefore, the dot-product of Eqs. (3) and (B2) gives the definition of speed V in the direction of flight in the flight path coordinate system:

$$\bar{V}\cdot\hat{t} = V = \frac{(\dot{r}_1^2 + \dot{r}_2^2 + \dot{r}_3^2)}{V} \tag{B3}$$

The final explicit form of momentum equations as given in Eqs. (8–10) is derived by taking the dot-product of Eqs. (A7) and (B1a,b,c), respectively. The force components are described in the flight-path coordinate system. Their contributions can be, therefore, superimposed on the final expressions.

Acknowledgment

The methodology described in this paper was developed in part under contract for the Air Force Wright Aeronautical Laboratories, F 33615-82-C-3002. The author expresses his appreciation to David T. Johnson and Capt. Louis Szabo of AFWAL/FIMG for their cooperation.

References

[1]Bauer, G. L., Cornick, D. E., Harper, A. R., Peterson, F. M., and Stevenson, R., "Program to Optimized Simulated Trajectories (POST)," Vol. II, *Utilization Manual*, NASA CR-132690, April 1975.

[2]Vinh, N. X., Busemann, A., and Culp, R. D., *Hypersonic and Planetary Entry Flight Mechanics*, The University of Michigan Press, Ann Arbor, MI, 1980, pp. 22–28.

[3]*Handbook of Astronautical Engineering*, edited by H. H. Koelle, McGraw-Hill, New York, 1961, pp. 6–29.

[4]Ikawa, H. and Rudiger, T. F., "Synergetic Maneuvering of Winged Spacecraft for Orbital Plane Change," *Journal of Spacecraft and Rockets*, Vol. 19, Nov.–Dec. 1982, pp. 513–520.

[5]*AFSCF Training Manual*, "Orbital Mechanics," Course No. 151, May 1982, pp. 1–33 to 1–39.